ANNALS OF PHYSICS 168, 1–26 (1986)

# Auxiliary Field Monte-Carlo for Quantum Many-Body Ground States*

G. SUGIYAMA† AND S. E. KOONIN

*W. K. Kellogg Radiation Laboratory, California Institute of Technology, Pasadena, California 91125*

Received July 2, 1985

We develop an algorithm for determining the exact ground state properties of quantum many-body systems which is equally applicable to bosons and fermions. The Schroedinger eigenvalue equation for the ground state energy is recast as a many-dimensional integral using the Hubbard–Stratonovitch representation of the imaginary-time many-body evolution operator. The integral is then evaluated stochastically. We test the algorithm for an exactly soluble boson system with an attractive potential and then extend it to fermions and repulsive potentials. Importance sampling is crucial to the success of the method, particularly for more complex systems. Computational efficiency is improved by performing the calculations in Fourier space. © 1986 Academic Press, Inc.

## 1. INTRODUCTION

Exact solutions to the many-body Schroedinger equation are of interest as benchmarks for testing approximation methods and Hamiltonians. The Green's Function Monte-Carlo (GFMC) [1, 2] and the related Diffusion Monte-Carlo (DMC) algorithms [3] accurately describe boson systems [2, 4] but allow only a restricted treatment of fermions. The many-body wavefunction is described by a statistically evolving set of configurations, each of which is specified by the coordinates of the particles. Antisymmetrization is therefore difficult to implement exactly with the simple local algorithms used to evolve the ensemble. This has prevented the unrestricted application of either the GFMC or DMC to fermion systems with more than four particles [5] or with state-dependent potentials, although the fixed-node approximation [3, 6] allows upper bounds on fermion ground state energies to be determined.

The Auxiliary Field Monte-Carlo algorithm (AFMC) discussed here [7] and the related method of coherent states [8, 9] allow an exact description of fermions by using a basis that consists of sets of single-particle wavefunctions. In the AFMC algorithm, the imaginary-time many-body propagator

$$U(T) = e^{-HT}$$

* Work supported in part by National Science Foundation Grants PHY82-17332 and PHY82-15500.

† Present address: Lawrence Livermore National Laboratory, Livermore, Calif. 94550.



0003-4916/86 $7.50

filters a trial function $\Phi$ to the exact ground state $\Psi$; that is, the ground state energy is given by

$$E_0 = \lim_{T\to\infty} \frac{\langle \Phi | HU(T) | \Phi \rangle}{\langle \Phi | U(T) | \Phi \rangle}. \tag{1}$$

The introduction of a trial function reduces statistical errors associated with the use of a finite ensemble of trajectories in the evaluation. $\Phi$ is, in principle, any wavefunction not orthogonal to $\Psi$. However, the method is tractable only if $\Phi$ is a symmetrized (antisymmetrized) product of single-particle orbitals for bosons (fermions).

The balance of this paper is arranged as follows. Section II details the AFMC algorithm. Applications to several test systems are described in Section III and Section IV discussed advantages and limitations of the method.

## 2. The AFMC Algorithm

### 2.1. *The Hubbard–Stratonovitch Transformation*

Our AFMC algorithm uses the Hubbard–Stratonovitch (HS) representation of the many-body propagator $U(T)$. Consider the general Hamiltonian

$$H = \sum_{\alpha\beta} K_{\alpha\beta}\rho_{\beta\alpha} + \frac{1}{2}\sum_{\alpha\beta\gamma\delta} v_{\alpha\beta\gamma\delta}\rho_{\gamma\alpha}\rho_{\delta\beta} \tag{2}$$

where

$$\rho_{\beta\alpha} \equiv a_\alpha^\dagger a_\beta$$

is the single-particle density operator and

$$K_{\alpha\beta} = T_{\alpha\beta} \pm \frac{1}{2}\sum_\gamma v_{\alpha\gamma\gamma\beta}$$

is the kinetic energy $T$ and a self-interaction term for bosons or fermions, which will be removed later. The subscripts $\alpha$, $\beta$, $\gamma$, and $\delta$ represent any internal degrees of freedom which may be present (such as spin, isospin, etc.), as well as the spatial coordinates. The HS transformation of the propagator $e^{-HT}$ introduces an auxiliary field to reduce the exponential of a two-body operator (e.g., the term involving $v$ in Eq. (2)) to a functional integral over an infinite set of exponentials of one-body operators. The transformation was originally developed to calculate the many-body partition function for systems containing two-body interactions [10]. It has been applied in Monte-Carlo calculations of the Hubbard model on a one-dimensional lattice [11] and has been used in approximate mean-field solutions of nuclear problems [12–14].

The HS representation of the propagator $U(T)$ is

$$U(t_f, t_i) = \int D[\sigma] \exp\left(\frac{1}{2}\int_{t_i}^{t_f} dt(\sigma, v\sigma)\right) U_\sigma(t_f, t_i), \tag{3a}$$

a coherent sum over an infinite set of operators $U_\sigma(T)$. Each $U_\sigma$ is the time-ordered product

$$U_\sigma \equiv T_t \exp\left(-\int_{t_i}^{t_f} dt\, h_\sigma(t)\right) \tag{3b}$$

describing evolution under the one-body Hamiltonian

$$\begin{aligned} h_\sigma(t) &= \sum_{\alpha\beta}\left[K_{\alpha\beta} + \sum_{\alpha'\beta'} \sigma_{\beta'\alpha'}(t)\, v_{\alpha'\alpha\beta'\beta}\right] \rho_{\beta\alpha}(t) \\ &\equiv \sum_{\alpha\beta} [K_{\alpha\beta} + W_{\alpha\beta}(t)]\, \rho_{\beta\alpha}(t). \end{aligned} \tag{3c}$$

The sum is weighted by the exponential, where we have used the shorthand notation

$$(\sigma, v\sigma) \equiv \sum_{\alpha'\beta'} \sigma_{\beta'\alpha'}(t)\, v_{\alpha'\alpha\beta'\beta} \sigma_{\beta\alpha}(t).$$

The HS transformation maps an interacting particle problem to a system of non-interacting particles coupled to a fluctuating time-dependent external field, $W_{\beta\alpha}$. The former particle interactions are mediated through the $\sigma$ field. We represent the many-body wavefunction $\Phi$ by a set of $A$ single-particle wavefunctions which propagate individually in the external potential. The AFMC method is in some respects similar to a formulation used in Monte-Carlo simulations of relativistic field theories [15]. In these problems, the fermion degrees of freedom are "integrated out," leaving only a boson theory with an effective action (analogous to the HS representation).

With the transformation of Eq. (3), we can rewrite the expression for the energy of Eq. (1) as a ratio of functional integrals:

$$E_0 = \lim_{T\to\infty} \frac{\int D[\sigma(x,t)] \exp\left(\frac{1}{2}\int_0^T (\sigma, v\sigma)\, dt\right) \langle \Phi |\, U_\sigma \,| \Phi \rangle \dfrac{\langle H\Phi |\, U_\sigma \,| \Phi \rangle}{\langle \Phi |\, U_\sigma \,| \Phi \rangle}}{\int D[\sigma(x,t)] \exp\left(\frac{1}{2}\int_0^T (\sigma, v\sigma)\, dt\right) \langle \Phi |\, U_\sigma \,| \Phi \rangle}. \tag{4}$$

After suitable discretization this integral expression can be evaluated numerically by Monte-Carlo methods.

2.2. *Discretization of the Integral*

To evaluate Eq. (4), the wavefunctions and fields must be discretized on a mesh. In one dimension, we bound space-time to a region $0 \leqslant t \leqslant T$, $|x| \leqslant L/2$ and define an $(N+1) \times M$ mesh

$$t_i = (i-1)\,\Delta t, \qquad i = 1,..., N+1, \quad \Delta t = T/N$$

$$x_j = \left(j - \frac{m}{2} - \frac{1}{2}\right)\Delta x, \qquad j = 1,..., M, \qquad \Delta x = L/M$$

with $M$ even. Of course, we suppose that $\Delta x$ and $\Delta t$ are sufficiently small so that effects from the discretization are less than statistical errors. Wavefunctions are defined on the mesh points, while the $\sigma$ field and one-body potential $W$ are given on the half time points, since they determine the evolution of $\Phi$ from one mesh time to the next. With the definition $\sigma_{ij} = \sigma(t_{i-1/2}, x_j)$, Eq. (4) can be discretized as:

$$E_0(T = N\,\Delta T) = \frac{\int D[\sigma_{ij}] \exp\left(\frac{1}{2}\sum_{i=1}^{N} (\sigma, v\sigma)_i\,\Delta t\right) \langle \Phi |\, U_\sigma \,| \Phi \rangle \dfrac{\langle H\Phi |\, U_\sigma \,| \Phi \rangle}{\langle \Phi |\, U_\sigma \,| \Phi \rangle}}{\int D[\sigma_{ij}] \exp\left(\frac{1}{2}\sum_{i=1}^{N} (\sigma, v\sigma)_i\,\Delta t\right) \langle \Phi |\, U_\sigma \,| \Phi \rangle}, \tag{5}$$

where the measure is

$$D[\sigma_{ij}] = \prod_{i=1}^{N} \prod_{j=1}^{M} d\sigma_{ij},$$

since constants vanish in the ratio, the inner product is

$$(\sigma, v\sigma)_i = \sum_{j=1}^{M} \sum_{k=1}^{M} \sigma_{ij} v_{jk} \sigma_{ik} (\Delta x)^2,$$

with $v_{jk} = v(x_j - x_k)$, and

$$U_\sigma = \prod_{i=1}^{N} U_\sigma^i,$$

describing one-body evolution from $t_i$ to $t_{i+1}$ under the single-particle Hamiltonian

$$h_{\sigma_i}(x_j) = -D^2/2m + \sum_{k=1}^{M} v_{jk} \sigma_{ik} (\Delta x)$$

($D^2$ is the usual 3-point discretization of the second derivative). We omit the self-energy term, $\pm\frac{1}{2}v(0)$, from $h_\sigma$, as this results in a constant shift of the energy scale for the time evolution which does not affect the right-hand side of Eq. (5).

From the standard derivation of the Hubbard–Stratonovich transformation by

discretizing the time evolution [12], it is clear that any approximation for $U_\sigma^i$ must be accurate through $O(\Delta t^2)$. We have used the Crank–Nicholson formula familiar from TDHF calculations [16],

$$U_\sigma(\Delta t) = \frac{(1 - \frac{1}{2}h_\sigma \Delta t/\hbar)}{(1 + \frac{1}{2}h_\sigma \Delta t/\hbar)}, \tag{6}$$

which has the further advantage of not amplifying those components of $\Phi$ associated with the largest-modulus eigenvalues of $h_\sigma$. The actual application of the Crank–Nicholson formula involves the inversion of a tridiagonal matrix. The usual Gaussian elimination and backward substitution recursion relations accomplish this efficiently in two sweeps through the mesh of size $M$ [17].

### 2.3. *Details of the Calculation*

The discretized expression for the energy is a form amenable to Metropolis Monte-Carlo evaluation [18]. To make this explicit, we rewrite the integral as

$$E_0 = \frac{\int D[\sigma_{ij}]\, P[\sigma_{ij}] \dfrac{\langle H\Phi |\, U_\sigma \,| \Phi \rangle}{\langle \Phi |\, U_\sigma \,| \Phi \rangle}}{\int D[\sigma_{ij}]\, P[\sigma_{ij}]}. \tag{7}$$

$E_0$ is the average of the energy estimator $\langle \Phi |\, HU_\sigma(T) \,| \Phi \rangle / \langle \Phi |\, U_\sigma(T) \,| \Phi \rangle$ over all field configurations, weighted by

$$P[\sigma] = \exp\left(\frac{1}{2}\sum_{i=1}^{N} (\sigma, v\sigma)_i \, \Delta t\right) \langle \Phi |\, U_\sigma \,| \Phi \rangle.$$

The Monte-Carlo evaluation of Eq. (7) is equivalent to many evolutions of the system in a random mean-field.

The Metropolis algorithm requires that $P[\sigma]$ be positive definite. This is satisfied by symmetrized product trial functions (bosons) and by spin- and/or isospin symmetric Slater determinants (fermions) interacting through a state-independent potential. If $P[\sigma]$ is not positive definite, $|P|$ can be used as the weight and the sign $P/|P|$ appended to the energy contribution from each configuration. However, even here $P$ must be predominantly of one sign for the denominator in Eq. (7) to remain large so that good statistical accuracy can be achieved. While we have no guarantee that $P$ is well-behaved in the general case, our results for fermion systems treated by the AFMC algorithm and by other methods [19] offer some encouragement on this point.

The integrals over $\sigma$ in Eq. (7) will not converge unless $(\sigma, v\sigma)_i$ is negative definite; i.e., the eigenvalues of $v_{jk}$ are all less than zero. This is equivalent to requiring that all Fourier components of $v(x)$ are negative. While this is certainly not true in general, it can often be guaranteed for a given $v$ by adding an appropriate two-

body interaction term to $H$. This makes the eigenvalues of the effective $v_{jk}$ negative definite and shifts $E_0$ in a trivial way (see Section 3.4).

An appropriate choice of the trial wavefunction can be determined through the use of approximate solutions or by using a physically likely basis set with parameters determined variationally. The initial configuration of the $\sigma$ field is taken to be the stationary phase approximation in the Hartree limit at all time slices:

$$\sigma_{\text{init}}(x_j, t_i) = \sigma_0(x_j) = \sum_{l=1}^{A} |\psi_l(x_j)|^2, \tag{8}$$

for all $t_i$. This is just the particle density; i.e., the mean-field generated by all of the particles in the static limit.

We update the $\sigma$ field for all space points at a single time value before the Metropolis acceptance/rejection test is applied. Energy contributions are calculated only after this has been done for all times; i.e., at the end of a sweep. There are two computational simplifications that result from this method of performing the Metropolis random walk. The weight function in discretized form is

$$P[\sigma] = \exp\left(\frac{1}{2}\Delta\tau \sum_{i=1}^{N} (\sigma, v\sigma)_i\right) \langle \Phi |\, U_N U_{N-1} \cdots U_i \cdots U_2 U_1 \,| \Phi \rangle$$

where $U_i \equiv e^{-h_\sigma(t_i)\Delta t}$ is the evolution operator from $t_i$ to $t_{i+1}$. Considering the exponential factor, it is evident that changes in the $\sigma$ field at a fixed time point $t_i$ affect only one term in the sum, giving a net contribution to $P[\sigma_{II}]/P[\sigma_I]$ of

$$\exp\left(-\frac{1}{2}\Delta\tau\left[\int dx\, dx'\, \sigma_I(x, t_i)\, v(x-x')\, \sigma_I(x', t_i) - \int dx\, dx'\, \sigma_{II}(x, t_i)\, v(x-x')\, \sigma_{II}(x', t_i)\right]\right);$$

the $\sigma$ fields at other time slices can be ignored.

A further gain in computational time is achieved by evolving the trial wavefunction $\langle \Phi |$ from the left once before the Monte-Carlo sweep begins and storing the resulting wavefunctions $\langle \Phi |\, U_N U_{N-1} \cdots U_i$ for all $i$. During the sweep, the "changed" fields $\sigma'$ are used to evolve the wavefunction forward, so that at any time $i$, the wavefunction $U'_{i-1} U'_{i-2} \cdots U'_1 \,| \Phi \rangle$ is known ($U'_i$ describes evolution under the "new" potential determined by $\sigma'$). Then, to perform one step in the Metropolis walk, only a single evolution, $U'_i$, and the calculation of two overlaps of already known wavefunctions

$$\frac{\langle \Phi |\, U_N \cdots U_{i+1}\, U'_i U'_{i-1} \cdots U'_1 \,| \Phi \rangle}{\langle \Phi |\, U_N \cdots U_{i+1} U_i U'_{i-1} \cdots U'_1 \,| \Phi \rangle},$$

are necessary to determine the matrix element contribution to the weight ratio.

To improve the efficiency of the Metropolis random walk, the AFMC algorithm incorporates a form of importance sampling—a biasing of the trajectories beyond that determined by the weight factor $W$. The trial sigma field $\sigma'$ is randomly generated from the old field by

$$\sigma_j'^{,i} = \sigma_j^i + \delta\eta_j \, \Delta\sigma \tag{9}$$

where $j$ and $i$ indicate points on the space-time mesh, $\delta$ is a uniformly distributed random number between $-1$ and 1, and $\Delta\sigma$ is a constant factor used to increase or decrease the overall size of the random steps. A reasonable choice for $\eta$ has been found to be the initial sigma field, $\sigma_0$, so that fractional changes are being made in the field. It turns out to be practical to choose $\Delta\sigma$ so that the Metropolis acceptance ratio is between 30 and 70%. This enables the $\sigma$ field distribution to converge to the asymptotic limit in a reasonable amount of computer time. Of course the precise value for $\Delta\sigma$ is highly dependent on the choice of the importance sampling scheme.

We perform error analysis assuming standard Gaussian statistics [20]. The energy estimators $E(v)$—the value after the $v$th sweep—must not be affected by the initial configuration of the $\sigma$ field. Therefore, a thermalization of $v_0$ sweeps is performed before contributions to the energy average ($\bar{E}$) are taken. For $v$ larger than $v_0$, $E(v)$ should differ from $\bar{E}$ by no more than expected statistical deviations. Once the initial relaxation has occurred, the precision of the energy estimate is increased by averaging at many subsequent times. Of course, for the averages to be meaningful and for the calculation of the standard deviation to be valid, statistically independent values must be used. Since each configuration is generated from the previous one, some correlations are to be expected. This can be taken into account by performing a sufficient number of sweeps, $\tau_{\text{corr}}$, between each contribution to the average. The correlation length $\tau_{\text{corr}}$ is determined by the number of sweeps for which the autocorrelation function of the energy estimators falls to less than 0.1. The relaxation times and correlation lengths are strongly affected by the choice of the importance sampling field $\eta$.

## 3. Results

### 3.1. *Bosons with a δ-function interaction*

For a first investigation, we have applied the AFMC method to a system which is exactly soluble and has been studied in some detail: $A$ bosons of mass $m$ in one dimension, interacting with each other through an attractive zero-range potential of strength $V_0$. The complete Hamiltonian is given by

$$H = \sum_{i=1}^{A} \frac{p_i^2}{2m} - \frac{1}{2} V_0 \sum_{i \neq j=1}^{A} \delta(x_i - x_j) + \frac{1}{2} mA\Omega^2 \left( \sum_i x_i/A \right)^2, \tag{10}$$

where we have added a harmonic oscillator of frequency $\Omega$ to confine the center-of-mass motion. This additional term contributes both one- and two-body pieces to $H$, and it is easy to show that the effective $(\sigma, v\sigma)$ is negative definite provided $\Omega < (6AV_0/mL^3)^{1/2}$. The oscillator frequency is also bounded from below by the requirement that the oscillator length, $(1/mA\Omega)^{1/2}$, be smaller than the mesh size, $L$, so that the mesh boundaries do not affect the solution. When this is satisfied, we are free to choose zero boundary conditions for the single-particle wavefunctions at $x = \pm L/2$.

The Hamiltonian (10) is exactly soluble for $\Omega = 0$ [21]; the eigenvalue of its only bound state is

$$E_0 = -A(A-1)(A+1)\, V_0^2 m/24.$$

The system can also be solved in the Hartree approximation provided that the oscillator term (which gives only a very small contribution to the Hartree energy for the parameters we have used) is not treated self-consistently. The Hartree energy and wavefunction are

$$E_{\mathrm{H}} = \pi^2 m\Omega^2 b^2/24A - A(A-1)^2\, V_0^2 m/24 \tag{11}$$

$$\Phi(x_1, \ldots, x_A) = \prod_{i=1}^{A} \sqrt{b/2}/\cosh bx_i \tag{12}$$

where $b = mV_0(A-1)/2$. This is the trial wavefunction we have used in the AFMC calculations. The spurious center-of-mass energy makes up exactly half of the difference between the Hartree and exact ground state energies ($\Omega = 0$), with all but 0.5% of the remaining gap accounted for by the leading term in the RPA chain [21].

The AFMC calculation is equivalent to that for a one-particle system: the many-body wavefunction consists of $A$ identical one-body functions propagating under identical operators $U_\sigma$. Only one single-particle wavefunction and one $\sigma$ field are required for the energy evaluation.

We chose physical units appropriate to nuclear systems, $\hbar^2/m = 41.47$ MeV-fm$^2$ and $V_0 = 41.47$ MeV-fm, and studied the $A = 6$-, 10-, and 20-particle systems. The parameters are given in Table I. We used a mesh of 30 spatial points and up to 160 time points. Standard checks on space and time discretizations were performed. Typical values of $\Delta t$ were on the order of $10^{-26}$–$10^{-25}$ s and $\Delta x$ was about 0.1 fm. The center-of-mass frequency was taken to be $\hbar\Omega = 25$ MeV, resulting in a shift of the exact ground state energy, $E_0$, by the zero-point energy, $\frac{1}{2}\hbar\Omega = 12.5$ MeV. To check that the system was properly confined by this potential, different choices of $\Omega$ were tested for total times $T$ in the asymptotic limit. The resulting values for the ground state energy $E(T)$ varied in the expected way.

Both the initial $\sigma$ field and the $\eta$ importance sampling field were set to the initial particle density. The size of changes in $\sigma$, weighted according to the initial field, ranged from $\Delta\sigma = 2.0$ to 5.0, for an acceptance ratio between 0.50 and 0.60. A ther-

TABLE I

Parameters for Systems of $A$ Bosons, Interacting through a Delta Function Potential

| $A$ | 6 | 6 | 10 | 10 | 20 | 20 |
|---|---|---|---|---|---|---|
| $\Delta t$ ($\times 10^{-25}$ s) | 1.0 | 2.5 | 0.5 | 1.0 | 0.05 | 0.10 |
| $N$ | 125 | 50 | 160 | 120 | 160 | 130 |
| $\Delta x$ (fm) | 0.15 | 0.15 | 0.10 | 0.10 | 0.04 | 0.04 |
| $M$ | 30 | 30 | 30 | 30 | 30 | 30 |
| $\hbar\Omega$ (MeV) | 25 | 25 | 25 | 25 | 25 | 25 |
| $\lambda$ (MeV) | −25.40 | −25.40 | −39.08 | −39.08 | −41.26 | −41.26 |
| $r_{\text{c.m.}}$ (fm) | 0.52 | 0.52 | 0.41 | 0.41 | 0.29 | 0.29 |
| $\Delta\sigma$ | 5.0 | 3.0 | 3.2 | 2.1 | 3.5 | 2.4 |
| $R_{\text{acc}}$ | 0.55 | 0.56 | 0.55 | 0.58 | 0.55 | 0.55 |
| $\tau_{\text{corr}}$ (trajectories) | 25 | 25 | 20 | 20 | 25 | 25 |
| $v_i$ (trajectories) | 1000 | 1000 | 1000 | 1000 | 1000 | 1000 |
| $v_f$ (trajectories) | 6000 | 6000 | 6000 | 6000 | 6000 | 6000 |

*Note.* The mesh was defined by $N\,\Delta t \times (M-1)\,\Delta x$, the harmonic oscillator by the frequency $\Omega$ with corresponding length $r_{\text{c.m.}}$, and the random walk by step size $\Delta\sigma$ yielding an acceptance ratio of $R_{\text{acc}}$. Energies were calculated every $\tau_{\text{corr}}$ trajectories from trajectory $v_i$ to $v_f$; $\lambda$ is the non-trivial eigenvalue of the potential.

malization interval of some 1000 sweeps was adequate and energies were taken over the next 5000 sweeps. The correlation length, $\tau_{\text{corr}}$, was 20–25 trajectories for the parameters chosen.

Results are shown in Figs. 1–3, in the form of plots of $E(T)$. The dashed and dotted lines indicate the Hartree and exact energies, respectively, including the harmonic oscillator contribution. Two energy estimators were used: the standard

$$\frac{\langle \Phi |\, H U_\sigma \,| \Phi \rangle}{\langle \Phi |\, U_\sigma \,| \Phi \rangle}$$

and the equivalent form with the Hamiltonian on the right,

$$\frac{\langle \Phi |\, U_\sigma H \,| \Phi \rangle}{\langle \Phi |\, U_\sigma \,| \Phi \rangle}.$$

For reference, results for a time step $\Delta t = 1.0 \times 10^{-25}$ s, where the discretization was slightly too coarse for proper evolution, are displayed in Fig. 2. The correct size for $\Delta t$ was determined by performing the AFMC with various size time steps and checking that the results converged to the same value.

In all three cases, $E(T)$ shows an initial relaxation and then asymptotically

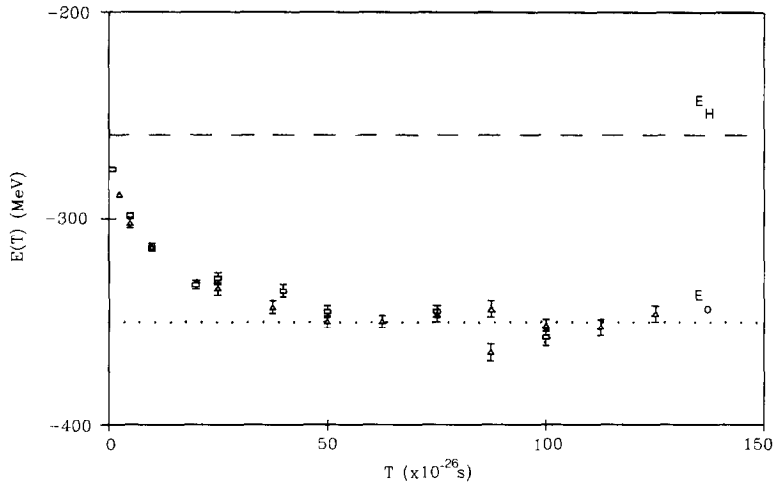


FIG. 1. $E(T)$ for 6 bosons interacting through a delta function potential. $E_H = -259.19$ is the Hartree energy and $E_0 = -350.36$ the exact ground state energy, including the center-of-mass harmonic oscillator. Two different time steps were used: $\square = 1.0 \times 1.0^{-25}$ s and $\Delta = 2.5 \times 10^{-25}$ s. Parameters are given in Table I.

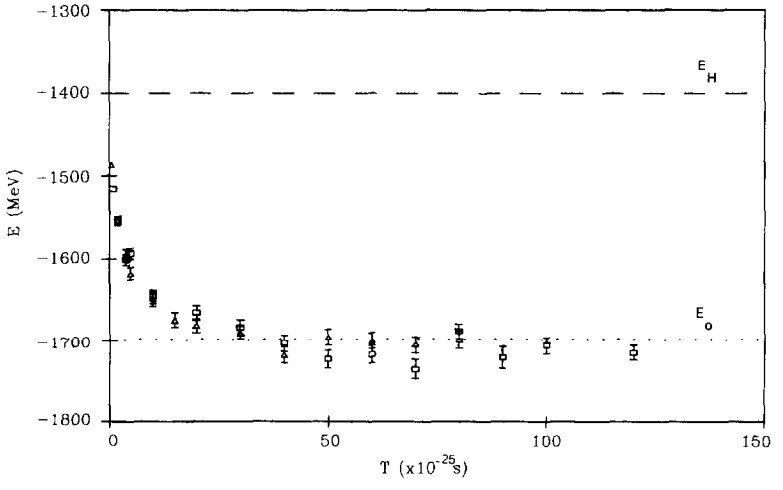


FIG. 2. $E(T)$ for 10 bosons interacting through a delta function potential. $E_H = -1399.61$ is the Hartree energy and $E_0 = -1698.14$ the exact ground state energy, including the center-of-mass harmonic oscillator. Two different time steps were used: $\square = 1.0 \times 10^{-25}$ s and $\Delta = 0.5 \times 10^{-25}$ s. Parameters are given in Table I.

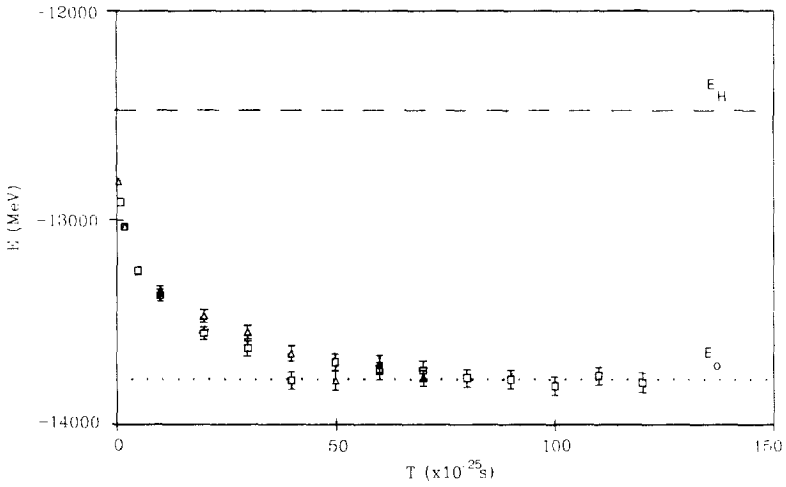


FIG. 3. $E(T)$ for 20 bosons interacting through a delta function potential. $E_H = -12475.6$ is the Hartree energy and $E_0 = -13776.3$ the exact ground state energy, including the center-of-mass harmonic oscillator. Two different time steps were used: $\square = 1.0 \times 1.0^{-26}$ s and $\Delta = 0.5 \times 10^{-26}$ s. Parameters are given in Table I.

approaches a value which fluctuates around the expected result for each $A$. This convergence becomes more rapid with increasing numbers of particles due to the spectrum of excited states; the energy gap to be resolved increases with increasing $A$. Consider Fig. 4, where the logarithm of the difference between $E(T)$ and its asymptotic value is plotted for $A = 10$. Two different relaxation scales are clearly seen. The rapid initial relaxation is related to the energy gap between the intrinsic ground state and the excited states. If the trial wavefunction $\Phi$ can be written approximately as a linear combination of the ground ($E_0$) and first excited state ($E_1$) consisting of $A-1$ bound particles plus one particle in the excited continuum at zero energy, then a plot of

$$\ln\left[\frac{E(T)-E_0}{E_H-E_0}\right]$$

as a function of time $T$ will have slope $-\Delta E = (E_1 - E_0)$. In Fig. 4, this slope is indicated by the dotted line. It is a lower bound on the relaxation, since other excited states also contribute. The dashed line is associated with the relaxation of the center-of-mass motion in the harmonic oscillator potential. While the asymptotic region is not reached for times $T$ used in the calculation, $T$ is long enough for the oscillator energy to be resolved within statistics.

These results provided an encouraging demonstration that the AFMC method could describe the ground state energy of a simple many-boson system. A typical calculation of some 60 time steps took 4 hours of CPU time on a VAX 11/750

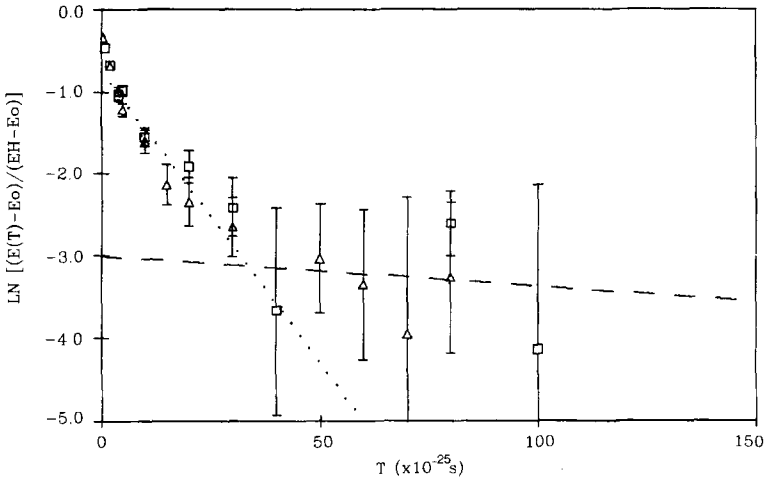


FIG. 4. Plot of $\ln[E(T)-E_0/E_H-E_0]$ for 10 bosons interacting through a delta function potential. Two different time steps were used: $\square = 1.0\times10^{-25}$ s and $\Delta = 0.5\times10^{-25}$ s. The dotted line shows the relaxation due to the energy gap between the ground and the first excited state. The second relaxation due to the center-of-mass oscillator is indicated by the dashed line. Parameters are given in Table I.

without floating point accelerator (about 5 minutes on a CDC 7600). It was noteworthy that the computational effort did not increase with the number of particles in the system.

### 3.2. *Fermions*

The AFMC formalism for fermion systems is straightforward. If the potential is independent of internal degrees of freedom, $v_{\alpha\beta}=v$, a total sigma field and density can be defined:

$$\bar{\sigma}(x)\equiv\sum_{\alpha}\sigma_{\alpha}(x) \tag{13a}$$

$$\bar{\rho}(x)\equiv\sum_{\alpha}\rho_{\alpha}(x), \tag{13b}$$

where the sums are over the internal degrees of freedom. In this case, the propagator written in terms of the redefined fields,

$$\begin{aligned} U&=\int D[\bar{\sigma}(x,t)]\, e^{(1/2)\int\bar{\sigma}(x)\,v(x-x')\,\bar{\sigma}(x')}\,U_{\bar{\sigma}} \\ U_{\bar{\sigma}}&=e^{-h_{\sigma}T}=T_t e^{-\int dt[K+\int dx\,dx'\bar{\sigma}(x)\,v(x-x')\,\bar{\rho}(x')]}, \end{aligned} \tag{14}$$

becomes formally identical in appearance to the case without internal variables. As in the boson case, only one $\sigma$ field is necessary—i.e., all the individual $\sigma_\alpha$ are subsumed in $\bar{\sigma}$, which determines the evolution of the trial wavefunction. For a more

general interaction, all the fields $\sigma_\alpha$ must be kept separately, each being used to evolve the corresponding single-particle wavefunctions independently—the problem then involves simultaneous solution of several coupled systems of the form considered here, one for each of the non-spatial degrees of freedom.

The fermion wavefunction was represented by a Slater determinant. Since there is nothing intrinsic to the propagator formulation or the Crank–Nicholson approximation that guarantees that fermion statistics will be preserved, we perform a Schmidt orthogonalization of the spatial states after each step of the time evolution. This orthogonalization is equivalent to a change of basis at each time step and guarantees exact antisymmetric of the wavefunction. The Metropolis weight factor and the energy estimator now involve calculations of determinants and inverses of $N \times N$ matrices [22], operations which can become very time-consuming for large systems involving few degeneracies.

For a test case of the fermion formalism we chose an exponential potential (i.e., a one-dimensional Yukawa potential):

$$v(x) = \frac{v_0}{2a} e^{-|x|/a}, \tag{15}$$

where $V_0$ is the strength and $a$ the range of the potential. The main computational complexity entailed by a finite-range interaction is the evaluation of the convolution integral

$$W(x) = \int v(x - x')\, \sigma(x')\, dx'.$$

For the exponential potential, however, this can be performed easily by noting that $W(x)$ satisfies a Helmholtz equation,

$$W''(x) - \frac{1}{a^2} W(x) = \frac{V_0}{a^2} \sigma(x),$$

which can be discretized as a tridiagonal matrix equation and solved by Gaussian elimination and backward substitution.

We chose a spin–isospin degenerate system. Such systems can be viewed as containing pairs of protons and neutrons with spin up and down. This choice has certain advantages. First, it allows a test of the combined field formalism of Eq. (13), Second, a larger number of particles are involved for the same amount of computer time, helping to ensure that the mean-field picture is valid. Indeed, attempts to apply the AFMC to systems of two particles fail to yield convergence with good statistics. Finally, the weight factor for a system with four spin–isospin degrees of freedom can immediately be seen to be positive definite, since all matrix elements are fourth powers of determinants of spatial overlap integrals and so are non-negative. This is not true a priori for non-degenerate fermions or for unfilled levels.

We took the constants for the potential to be $V_0 = 41.47$ MeV-fm and $a = 0.8$ fm, values of typical nuclear strengths and ranges. Systems of 4, 8, and 12 particles were treated, corresponding to 1 (bosons), 2, and 3 spatial orbitals. Table II contains the sets of parameters we used. Mesh sizes varied from 40 to 60 points, with the spatial lattice becoming slightly more closely spaced and extended in range ($\Delta x \approx 0.20$–$0.25$ fm) for the multiple level systems. Time lattices of up to 160 points were used, with at least two values of $\Delta t$ tested for each system, ranging between $10^{-25}$ and $10^{-24}$ s. We verified that our results did not depend on the discretization. Standard checks on the results were made as described previously.

As before, a harmonic oscillator potential was added to the Hamiltonian to confine the center-of-mass. This makes an exact determination of the eigenvalues of the total potential difficult. However, the requirement that the exponent $(\sigma, v\sigma)$ be negative definite can still be met if the strength of the harmonic oscillator is not too great. For the system we studied, $\hbar\Omega$ was taken to be 10 MeV and the sign of the exponent was checked explicitly during the calculation.

The trial wavefunction $\Phi$ was given by a Slater determinant of orthogonal states in a harmonic oscillator potential, the length parameter, $\beta$, set variationally to minimize the energy (omitting the center-of-mass oscillator potential). As a check on the trial wavefunction and on the energy convergence, the AFMC was also run

TABLE II

Parameters for $A$ Spin–Isospin Degenerate Fermions Interacting through an Exponential Potential

| $A$ | 4 | 4 | 4 | 8 | 8 | 12 | 12 |
|---|---|---|---|---|---|---|---|
| $\Delta t (\times 10^{-25}$ s) | 20.0 | 40.0 | 40.0 | 2.5 | 5.0 | 2.5 | 5.0 |
| $N$ | 50 | 70 | 70 | 140 | 100 | 160 | 100 |
| $\Delta x$ (fm) | 0.25 | 0.25 | 0.25 | 0.20 | 0.20 | 0.20 | 0.20 |
| $M$ | 40 | 40 | 40 | 50 | 50 | 70 | 70 |
| $\hbar\Omega$ (MeV) | 10 | 10 | 10 | 10 | 10 | 10 | 10 |
| $r_{\text{c.m.}}$ (fm) | 1.0 | 1.0 | 1.0 | 0.72 | 0.72 | 0.59 | 0.59 |
| Trial wavefunction | $g$ | $g$ | $c$ | $g$ | $g$ | $g$ | $g$ |
| $\beta$ (fm) | 1.4 | 1.4 | 0.9 | 1.4 | 1.4 | 1.6 | 1.6 |
| $\Delta\sigma$ | 8.0 | 6.0 | 5.5 | 14.0 | 11.0 | 12.0 | 8.0 |
| $R_{\text{acc}}$ | 0.50 | 0.50 | 0.50 | 0.55 | 0.55 | 0.51 | 0.50 |
| $\tau_{\text{corr}}$ (trajectories) | 25 | 25 | 25 | 25 | 25 | 25 | 20 |
| $v_i$ (trajectories) | 1000 | 1000 | 1000 | 1000 | 1000 | 1000 | 1000 |
| $v_f$ (trajectories) | 6000 | 6000 | 6000 | 6000 | 3000 | 3000 | 3000 |

*Note.* The mesh was defined by $N\Delta t \times (M-1)\Delta x$, the harmonic oscillator by the frequency $\Omega$ with length $r_{\text{c.m.}}$, and the random walk by the step size $\Delta\sigma$ yielding an acceptance ratio of $R_{\text{acc}}$. Energies were calculated every $\tau_{\text{corr}}$ trajectories from trajectory $v_i$ to $v_f$. The trial wavefunction was specified to be a determinant of either the harmonic oscillator ($g$) or delta function solutions ($c$) with parameter $b = \beta^{-1}$.

for the 4-boson system using the trial wavefunction $1/\cosh(bx)$, the Hartree wavefunction for the delta function potential. The initial $\sigma$ field and the $\eta$ field were once again taken to be the initial particle density.

Results are shown as plots of $E(T)$ in Figs. 5–8 for the 4-, 8-, and 12-particle systems. Variational energies for the trial wavefunction, including the center-of-mass oscillator contribution, are indicated by the dotted lines. Note that in all cases the asymptotic energies include a 5-MeV contribution from the center-of-mass oscillator. All plots show the same initial relaxation and asymptotic approach to a limiting energy around which the remaining points fluctuate, as in the previous boson case. Figure 6 compares the results for the two different trial wavefunctions; both provide a quick resolution to the same ground state energy. Typical values of $\tau_{\text{corr}}$ were 20–25 trajectories, as in the delta function case, implying that the spatial range of the potential did not translate into longer correlation lengths. The initial relaxation was taken to be 1000 sweeps, with energies taken over the next 2000.

The total time needed to resolve the ground state energy was roughly $T = \hbar/E_0$ in all three cases—i.e., $T$ was shorter for the systems with more particles and larger binding energies. The number of discrete time steps was comparable to that in the boson case, so that the computational time was increased only by the additional time needed to evaluate the convolutions and a multiplicative factor depending on the number of orbital states involved. Typical computational times for the 3-level system were on the order of 6 hours of CPU time for the same VAX 11/750 with floating point accelerator.

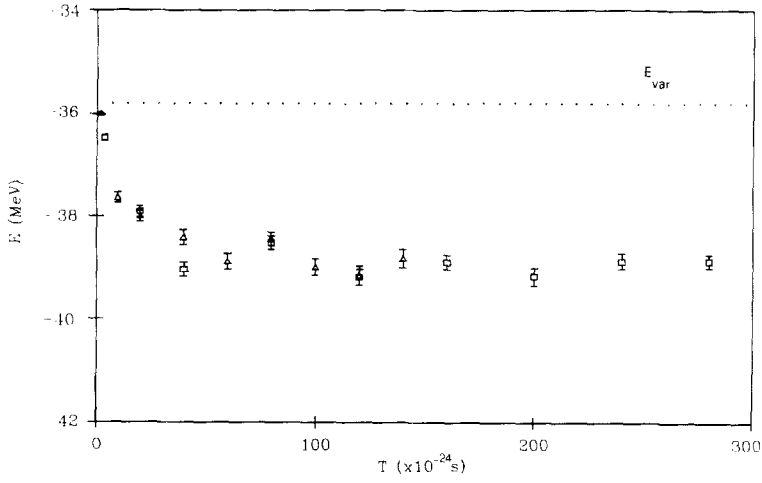


FIG. 5. $E(T)$ for 4 spin–isospin degenerate fermions interacting through an exponential potential. $E_{\text{var}} = -35.8$ MeV is the variational energy. Two different time steps were used: $\square = 4.0 \times 10^{-24}$ s and $\Delta = 2.0 \times 10^{-24}$ s. Parameters are given in Table II.

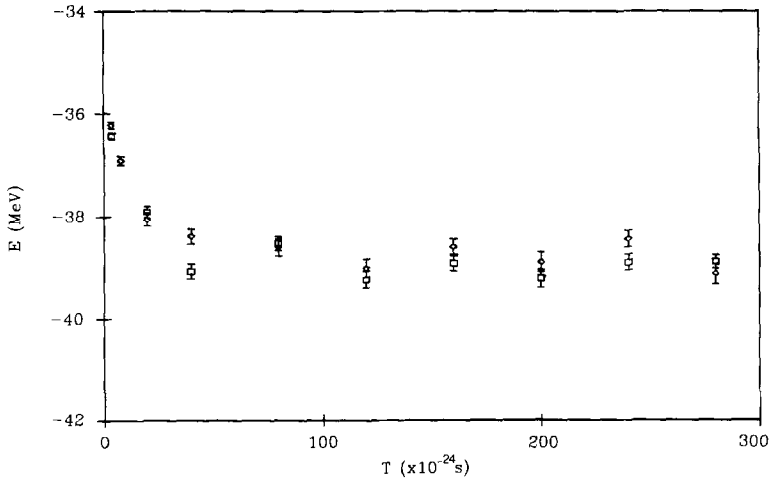


FIG. 6. $E(T)$ for 4 spin–isospin degenerate fermions interacting through an exponential potential. $E_{\text{var}} = -35.8$ MeV is the variational energy. Two different trial wavefunctions were used: □ = harmonic oscillator and $\Delta$ = delta function solution with the size of the time step being $4.0 \times 10^{-24}$ s in both cases. Parameters are given in Table II.

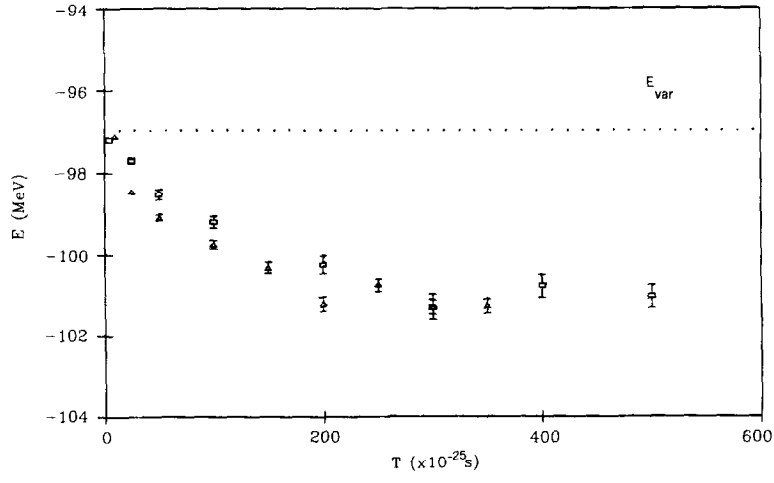


FIG. 7. $E(T)$ for 8 spin–isospin degenerate fermions interacting through an exponential potential. $E_{\text{var}} = -96.5$ MeV is the variational energy. Two different time steps were used: □ = $5.0 = 10^{-25}$ s and $\Delta = 2.5 \times 10^{-25}$ s. Parameters are given in Table II.

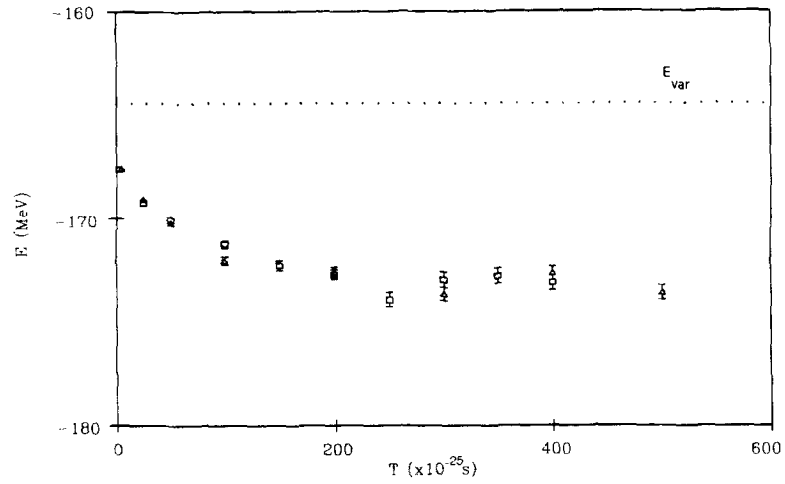


FIG. 8. $E(T)$ for 12 spin–isospin degenerate fermions interacting through an exponential. $E_{var} = -164.4$ MeV is the variational energy plus non-self-consistent center-of-mass harmonic oscillator energy. Two different time steps are used: $\square = 2.5 \times 10^{-25}$ s and $\Delta = 5.0 \times 10^{-25}$ s. Parameters are given in Table II.

### 3.3. *Sampling σ in Fourier Space*

Several considerations suggest an improvement to the Auxiliary Field Monte-Carlo method discussed so far. The method used in the previous sections has the disadvantage of resulting in extremely irregular $\sigma$ fields. This is caused not by insufficient resolution in the space discretization, but rather is due to the Metropolis walk itself, in which random, uncorrelated changes are made at every mesh point. The physical system is not expected to fluctuate on this scale. Moreover, the integrability of such extremely erratic functions becomes rather questionable. The spatial algorithm also appears somewhat inefficient, as can be seen by considering the nature of the importance sampling field $\eta$. This suggests that a faster random walk might be generated by making *correlated* changes of the field at all space points at one time slice.

We have therefore investigated an alternative algorithm using a Fourier decomposition of the fields and propagator:

$$\sigma(x, t) = \sum_{q=1}^{M-1} \sin(2q\pi x/L)\, \sigma_q(t), \qquad |x| < L/2 \tag{16}$$

$$U(T) = \int D[\sigma(k)] \exp\left( \int_0^T dt \frac{1}{2} \sum_k \sigma^*(k, t)\, v(k)\, \sigma(k, t) \right)$$

$$\times \exp\left( -\int_0^T dt \sum_k \sigma^*(k, t)\, v(k)\, \rho(k, t) \right), \tag{17}$$

where $\rho(k)$ is the density operator and $D[\sigma(k)]$ is the measure of integration. The sine decomposition imposes zero boundary conditions on the $\sigma$ field at the ends of the mesh. The wavefunctions were again simple products (bosons) or Slater determinants (fermions), expressed in terms of their Fourier components. In actual calculations, a fast Fourier transform rather than a sine series decomposition was used.

The Metropolis random walk was performed using an importance sampling field $\eta_q$ which weighted Fourier components of $\sigma$ rather than its values at individual mesh points. Since it seemed likely that only the low- and intermediate-frequency components of $\sigma$ contribute significantly to the evolution, calculations were made with $\sigma_q$ fixed ($\eta_q = 0$) for $q > N_q$; $N_q$ was then increased until the energy remained the same within statistical errors.

The spatial and Fourier AFMC importance sampling algorithms were compared for the case of 10 bosons interacting with the exponential potential of the previous section. Table III lists the various parameters used. The mesh contained 64 space points with $\Delta x = 0.15$ fm and up to 180 time steps of size $\Delta t = 5.0 \times 10^{-25}$ s. The

TABLE III

Parameters for $A = 10$ Bosons Interacting through an Exponential Potential

| | Spatial importance sampling | Fourier importance sampling $\eta_q \approx \eta_q^{\text{trial}}$ |
|---|---|---|
| $\Delta t$ ($\times 10^{-25}$ s) | 5.0 | 5.0 |
| $N$ | 160 | 140 |
| $\Delta x$ (fm) | 0.15 | 0.15 |
| $M$ | 64 | 64 |
| $\hbar\Omega$ (MeV) | 10.0 | 10.0 |
| $r_{\text{c.m.}}$ (fm) | 0.65 | 0.65 |
| $\beta$ (fm) | 1.5 | 1.5 |
| $N_q$ | All space points changed | 10 |
| $\Delta\sigma$ | 8.5 | 27.0 |
| $R_{\text{acc}}$ | 0.53 | 0.56 |
| $\tau_{\text{corr}}$ (trajectories) | 40 | 40 |
| $\nu_i$ (trajectories) | 1000 | 1000 |
| $\nu_f$ (trajectories) | 3000 | 3000 |

*Note.* The mesh is defined by $N\Delta t \times (M-1)\Delta x$, the harmonic oscillator by the frequency $\Omega$ with length $r_{\text{c.m.}}$, and the random walk by the step size $\Delta\sigma$ yielding an acceptance ratio of $R_{\text{acc}}$. Energies were calculated every $\tau_{\text{corr}}$ trajectories from trajectory $\nu_i$ to $\nu_f$. The harmonic oscillator trial function parameter is $\beta$. The importance sampling schemes used are indicated, with only the lowest $N_q$ frequencies involved in the random walk.

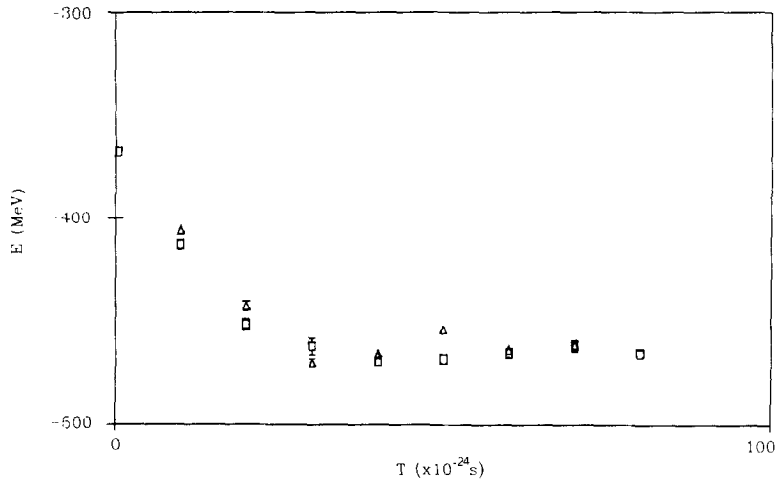


FIG. 9. Comparison of $E(T)$ for spatial and Fourier space importance sampling for a system of 10 bosons interacting through an exponential potential. The points □ indicate spatial sampling while Δ indicates Fourier decomposition sampling with frequency importance sampling given by the trial wavefunction. Parameters are given in Table III.

center-of-mass harmonic oscillator was chosen to have strength $\hbar\Omega = 10$ MeV and the trial function was taken to be a product of harmonic oscillator basis states with the length parameter determined variationally. Energies were calculated over 2000 trajectories after a relaxation of 1000 sweeps.

Results are shown as Fig. 9 as a plot of $E(T)$. Note that the center-of-mass harmonic oscillator shifts the true ground state energy by 5 MeV. Both calculations yielded the same ground state energy, with a total time for convergence on the order of $4.0 \times 10^{-23}$ s. Correlation lengths were not significantly different for the two methods—statistical independence was assured by calculating the energy estimators only every 40 sweeps of the mesh.

A considerable gain in CPU time was possible working in Fourier component space by eliminating the convolution integrals in the potential. The spatial convolution took about 50% of the CPU time (more in the case of more complicated interactions). There was also an improvement in efficiency for Fourier importance sampling because only the 10 lowest Fourier components had to be updated to obtain the results shown, rather than $\sigma$ values at each of the 60 mesh points. The limit on $N_q$ we found implied that significant length scales were on the order of 1.0–2.0 fm—a reasonable result for an exponential potential of range 0.8 fm. Overall, the Fourier space calculations were about twice as fast as those of the spatial algorithm.

The case of 12 spin–isospin degenerate fermions with an exponential interaction, calculated earlier, was treated by various Fourier decomposition algorithms and the

TABLE IV

Parameters for $A = 12$ Spin–Isospin Degenerate Fermions Interacting through an Exponential Potential

| | Spatial importance sampling | Fourier importance sampling $\eta_q \approx \sigma_q^{\text{trial}}$ | Fourier importance sampling $\eta_q \approx 1$ |
|---|---|---|---|
| $\Delta t$ ($\times 10^{-25}$ s) | 2.5 | 2.5 | 2.5 |
| $N$ | 160 | 100 | 120 |
| $\Delta x$ (fm) | 0.20 | 0.22 | 0.22 |
| $M$ | 70 | 64 | 64 |
| $\hbar\Omega$ (MeV) | 10.0 | 10.0 | 10.0 |
| $r_{\text{c.m.}}$ (fm) | 0.59 | 0.59 | 0.59 |
| $\beta$ (fm) | 1.6 | 1.6 | 1.6 |
| $N_q$ | All space points changed | 10 | 10 |
| $\Delta\sigma$ | 12.0 | 32.0 | 16.0 |
| $R_{\text{acc}}$ | 0.51 | 0.52 | 0.52 |
| $\tau_{\text{corr}}$ (trajectories) | 25 | 125 | 18 |
| $v_i$ (trajectories) | 1000 | 1000 | 1000 |
| $v_f$ (trajectories) | 3000 | 3000 | 3000 |

*Note.* The mesh was defined by $N\,\Delta t \times (M-1)\,\Delta x$, the harmonic oscillator by the frequency $\Omega$ with length $r_{\text{c.m.}}$, and the random walk by the step size $\Delta\sigma$ yielding an acceptance ratio of $R_{\text{acc}}$. Energies were calculated every $\tau_{\text{corr}}$ trajectories from trajectory $v_i$ to $v_f$. The harmonic oscillator trial function parameter was $\beta$. The importance sampling schemes used are indicated, with only the lowest $N_q$ frequencies involved in the random walk.

results were compared. Parameters are given in Table IV for the spatial and two Fourier importance sampling functions:

$$\eta_q = |\sigma_q^{\text{trial}}|, \qquad q < N_q \tag{18a}$$

and

$$\eta_q = 1.0, \qquad q < N_q. \tag{18b}$$

The mesh parameters, the trial wavefunction, and the initial condition on the $\sigma$ field were as described previously.

Energies calculated over 2000 trajectories after a 100 trajectory thermalization are shown in Fig. 10. Note that the actual ground is 5 MeV lower, after the contribution from the center-of-mass oscillator is removed. Only the 10 lowest frequencies were used in the Fourier space calculations ($N_q = 10$). Convergence to the asymptotic energy occurred after a total time $T = 3.0 \times 10^{-23}$ s for spatial importance sampling and for the Fourier weighting field of Eq. (18b).

The correlation lengths for the three choices of importance sampling showed significant differences. For $\eta_q = 1$, $\tau_{\text{corr}} = 18$ sweeps, they were some 30% smaller

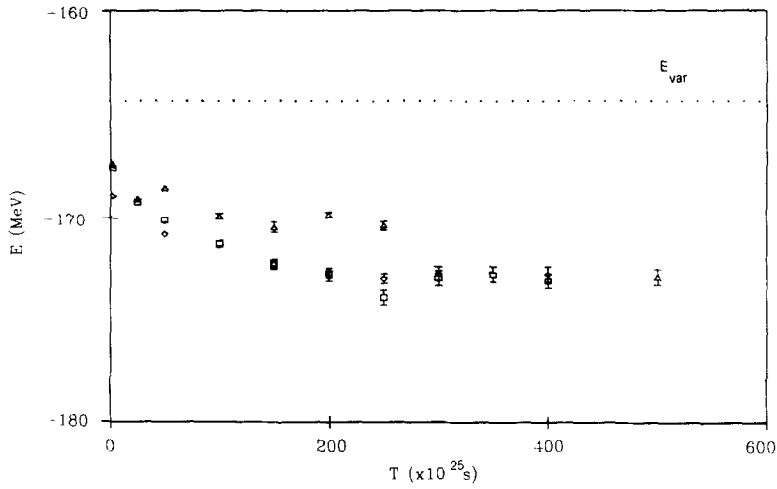


FIG. 10. $E(T)$ for 12 spin–isospin degenerate fermions interacting through an exponential potential. The □ points are identical to those in Fig. 8, and the $\Delta$ and the diamonds show Fourier decomposition sampling with $1/q$ and uniform frequency importance sampling, respectively. All three used a time step of $2.5 \times 10^{-25}$ s. Parameters are given in Table IV.

than for the spatial weighting method and 80% less than for the case $\eta_q = \sigma_q^{\text{trial}}$. This implied that the importance sampling field of Eq. (18a) was a poor choice. In fact, it is apparent from Fig. 10 that thermalization was not achieved for a small number of time steps, which is not surprising, as a relaxation period of only eight correlation lengths (1000 trajectories) was used.

The sigma fields remained erratic, though slightly smoother than before. However, an examination of the one-body potential showed a set of roughly symmetrically situated potential wells, reflecting the density of the three spatial orbitals.

These two examples indicate the critical nature of importance sampling in establishing an efficient algorithm. A Fourier space scheme using a proper choice of $\eta_q$ produces a significantly faster random walk, by changing Fourier components rather than individual field values. In general, the autocorrelation test eliminates the worst choices for the importance sampling field. However, it does not indicate the optimal choice of $\eta$, since it cannot distinguish between schemes changing the field at single points and those performing spatially correlated changes.

### 3.4. *Repulsive Potentials*

The application of the AFMC algorithm to systems involving repulsive potentials has an additional difficulty due to the negativity condition on the inner product $(\sigma, v\sigma)$ in the Metropolis exponent (see Eq. (4)). For systems containing repulsive potentials, it may not be possible to satisfy this condition for any choice of $\Omega$. We have considered two methods for dealing with such systems.

The first uses the same formulation as before, adding an appropriate two-body interaction term to the Hamiltonian to ensure that the eigenvalues of the resulting

effective potential are negative definite. Consider the effect of an additional potential which does not affect the energy:

$$V_{\alpha\beta}^{\text{add}}(x, x') = C\delta_{\alpha\beta}\,\delta(x-x'), \tag{19}$$

where $C$ is some constant. This potential contributes a term in $\int dx \sum_\alpha C\sigma_\alpha(x)\,\rho_\sigma(x)$ in $h_\sigma$ and an additional term to the exponent in the Metropolis weight

$$(\sigma, v\sigma)^{\text{add}} = C\int dx \sum_\alpha \sigma_\alpha^2(x).$$

Since this has the sign of $C$, by choosing the strength of the potential to be sufficiently negative, the exponent can be forced to satisfy the negativity condition. Bosons can be incorporated into the formalism by treating them as fermions with $A$ internal degrees of freedom.

To test this method, we chose a system which has been solved using standard techniques in a study of meson–nucleon field theory [23]. For static baryons, the scalar and vector meson interactions reduce to the sum of attractive and repulsive Yukawa potentials that reproduce the basic features of the nucleon–nucleon force. In one dimension, the static potential is given by

$$v(x) = \frac{1}{2}\left[\frac{g_{\text{V}}^2}{m_{\text{V}}}\,e^{-m_{\text{V}}|x|} - \frac{g_{\text{S}}^2}{m_{\text{S}}}\,e^{-m_{\text{S}}|x|}\right] \tag{20}$$

with $g_{\text{V}}$, $g_{\text{S}}$ the vector and scalar coupling constants and $m_{\text{V}}$, $m_{\text{S}}$ the meson masses. The parameters were set to provide a reasonable nucleon–nucleon potential with a repulsive core, $V(x=0)>0$, and a typical nuclear core radius of $x_{\text{c}} = 0.4$ fm (defined by $V(x_{\text{c}}) = 0$). The range of the potentials were fixed by the mass of the pion, $m_{\text{S}} = m_\pi = 140$ MeV, and the omega meson, $m_{\text{V}} = m_\omega = 783$ MeV. The binding energy per particle for nuclear matter in the mean-field approximation was taken to be 16 MeV at saturation. These considerations were sufficient to specify $g_{\text{S}} = 196$ MeV and $g_{\text{V}} = 890$ MeV.

Table V lists the parameters of a system of four non-degenerate fermions interacting through this potential. The calculation was performed using both spatial and Fourier importance sampling. The mesh consisted of 150 points of spacing $\Delta x = 0.08$ fm, the time interval was $\Delta t = 1.0 \times 10^{-24}$ s, and up to 60 time steps were used. All standard tests on the parameters were performed. The same trial wavefunction was used as for the purely attractive potential and the initial configuration of the $\sigma$ field was again taken to be the trial particle density, as was the importance sampling field. Only the 15 lowest-frequency components in the Fourier decomposition of $\sigma$ were changed during the random walk. Results were checked to be the same within statistical errors when more components were included.

The results shown in Fig. 11 are in agreement with the value obtained in [23], $E_0 = -64.7 \pm 0.7$ MeV, when the 1-MeV center-of-mass oscillator energy is taken into account. Both importance sampling schemes converge to the asymptotic energy

TABLE V

Parameters for $A = 4$ Fermions Interacting through an Attractive and Repulsive Exponential Potential

| | Spatial importance sampling | Fourier importance sampling $\eta_q \approx \sigma^{\text{trial}}$ |
|---|---|---|
| $\Delta t$ ($\times 10^{-24}$ s) | 1.0 | 1.0 |
| $N$ | 100 | 100 |
| $\Delta x$ (fm) | 0.08 | 0.09 |
| $M$ | 150 | 128 |
| $\hbar\Omega$ (MeV) | 2.0 | 2.0 |
| $r_{\text{c.m.}}$ (fm) | 2.3 | 2.3 |
| $\beta$ (fm) | 1.3 | 1.3 |
| $N_q$ | — | 15 |
| $\Delta\sigma$ | 3.5 | 3.0 |
| $R_{\text{acc}}$ | 0.54 | 0.52 |
| $\tau_{\text{corr}}$ (trajectories) | 45 | 30 |
| $v_i$ (trajectories) | 1000 | 1000 |
| $v_f$ (trajectories) | 3000 | 3000 |
| $V_{\text{add}}$ (MeV) | −200 | −200 |

*Note.* The mesh was defined by $N\Delta t \times (M-1)\Delta x$, the harmonic oscillator by the frequency $\Omega$ with length $r_{\text{c.m.}}$, and the random walk by the step size $\Delta\sigma$ yielding an acceptance ratio of $R_{\text{acc}}$. Energies were calculated every $\tau_{\text{corr}}$ trajectories from trajectory $v_i$ to $v_f$. The harmonic oscillator trial function parameter is $\beta$. The importance sampling schemes used are indicated, with only the lowest $N_q$ frequencies involved in the random walk. $V_{\text{add}}$ is the strength of the additional potential required by the negativity condition on the Metropolis exponent.

in a time on the order of $T = 1.0 \times 10^{-22}$ s. However, the results from the spatial weighting process fluctuate considerably. The value of $T$ suggests that an energy gap on the order of 10 MeV is being resolved; however, this is only a rough estimate as there is no way of identifying the various excited states for this interaction. We found a significant difference in the correlation lengths for the two importance sampling methods: the spatial weighting scheme had $\tau_{\text{corr}}$ half again as large as that for the $\eta_q$ case. This was another indication that Fourier importance sampling was more efficient. Further, in this sampling scheme, the one-body potential was a relatively smooth function showing several symmetrically placed barriers separating potential wells where the particle density concentrated. The center-of-mass oscillator compressed the overall radius and increased the density in the center.

The CPU time required for the Fourier sampling calculation was 12 hours on the VAX 11/750 with floating point accelerator and roughly twice that for spatial importance sampling. The major difficulty with extending this calculation to

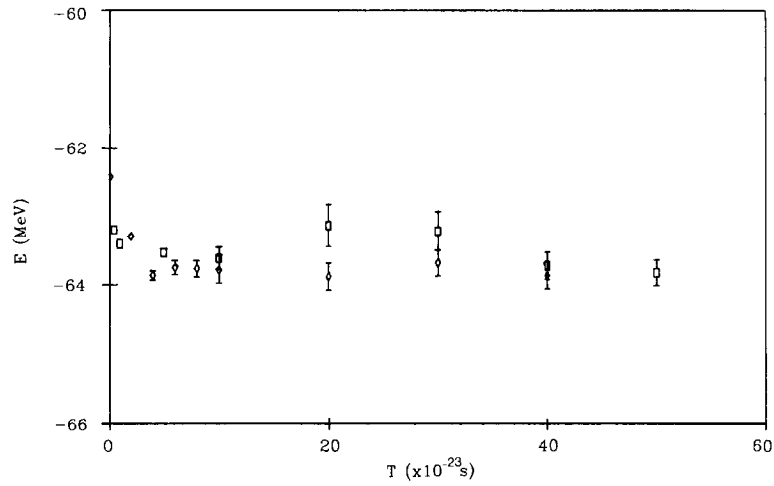


FIG. 11. $E(T)$ for 4 fermions interacting through a combined attractive and repulsive exponential. The time steps were: $\square = 1.0 \times 10^{-26}$ s with the changes in the $\sigma$ field performed using Fourier decomposition importance sampling given by the trial wavefunction, and $\Delta = 2.5 \times 10^{-26}$ s using spatial sampling. Parameters are given in Table V.

systems containing more particles is that computer time is proportional to the number of particles, even for systems with internal degrees of freedom. However, the convergence and statistics are expected to be better for such systems.

Our second method for treating repulsive potentials uses a formulation involving complex fields. The extra degree of freedom provided by the imaginary part of the field allows the construction of the exponential factor $(\sigma, v\sigma)$ in such a way as to satisfy the negativity condition. The energy is then calculated using the expression

$$E_0 = \lim_{T \to 0} \frac{\int D[\sigma, \sigma^*]\, e^{(1/2)\int (\sigma, v\sigma)} \left[ |\langle \Phi |\, U_\sigma \,| \Phi \rangle| \dfrac{\mathrm{Re}\langle \Phi |\, H U_\sigma \,| \Phi \rangle}{|\langle \Phi |\, U_\sigma \,| \Phi \rangle|} \right]}{\int D[\sigma, \sigma^*]\, e^{(1/2)\int (\sigma v \sigma)} |\langle \Phi |\, U_\sigma \,| \Phi \rangle| \dfrac{\mathrm{Re}\langle \Phi |\, U_\sigma \,| \Phi \rangle}{|\langle \Phi |\, U_\sigma \,| \Phi \rangle|}}, \tag{21}$$

an expression for the ground state energy as a ratio of the average of two quantities—the energy estimator $\langle \Phi |\, H U_\sigma \,| \Phi \rangle / |\langle \Phi |\, U_\sigma \,| \Phi \rangle$ and the signature estimator $\langle \Phi |\, U_\sigma \,| \Phi \rangle / |\langle \Phi |\, U_\sigma \,| \Phi \rangle|$. We tried this algorithm with both the spatial and the Fourier decomposition importance sampling schemes. The results were not good; approximate energies were obtained but with poor statistics. This was due to cancellations in the denominator integral. Apparently, to use this scheme, a more clever importance sampling for biasing the random walk is necessary.

## 4. DISCUSSION

The auxiliary field formalism provides a method for determining the exact ground state energies of many-body systems. In principle, the numerical techniques

we have developed can be used to solve systems with a variety of interactions. In practice, of course, there are limits imposed by the amount of computer time required. We tested the AFMC on several boson and fermion systems in one dimension, involving both attractive and repulsive potentials. While the formalism is identical in both cases, an antisymmetrization procedure was used for fermions to maintain proper statistics. The ground states energies found show good agreement in cases where results are known from other techniques, whether exact solutions or other Monte-Carlo values. They are an encouraging demonstration that the AFMC algorithm can be applied to a number of many-body systems.

A principal advantage of the AFMC method is its proper treatment of fermions. The HS representation of the propagator allows the system to be described by a set of single-particle wavefunctions for which antisymmetrization can be enforced exactly—a property not shared by the GFMC and DMC algorithms. However, whether or not the AFMC will be able to resolve ground state energies more accurately than the other Monte-Carlo methods for systems of physical interest remains an open question.

Our results for various systems make it clear that, as in other Monte-Carlo methods for many-body ground states, importance sampling is critical to obtaining efficient convergence and good statistics. A poor choice of the weighting function $\eta$ causes extremely long correlation and thermalization times and makes calculations impractical. A choice for $\eta$ based on the trial wavefunction is generally adequate for simple systems, though not necessarily optimal. The "trick" is to build into the method as much as possible of the physics without biasing the results by limiting the degrees of freedom of the system.

The proper treatment of fermion statistics in the AFMC is balanced by the need to specify wavefunctions and fields over all space and time, rather than just the coordinates of each particle. If the wavefunction is defined on a spatial mesh, the number of lattice points becomes prohibitive. This is especially true in several dimensions where meshes become extremely large, unless there is symmetry so that various spatial degrees of freedom can be integrated out. However, sampling of the Fourier components of the field appears to circumvent this problem, at least for regular potentials with Fourier transforms, since it can eliminate the need for a spatial lattice. This method is also more efficient, since the Fourier space random walk involves only the physically important lowest-frequency components. This provides some hope that more complicated systems can be treated with the AFMC. However, the representation of the many-body wavefunction as a set of single-particle orbitals may make it impossible to deal with potentials with a very strong repulsive core, since a determinantal form for the wavefunction is not a good approximation to the exact eigenstate in these cases.

Recently, progress has been made in developing functional integral techniques for nuclear physics using a variety of representations of the evolution operator [8, 14, 24]. Other than its exact enforcement of antisymmetrization, the AFMC possesses one significant and perhaps crucial advantage—it is the only form that allows the energy integral to be cast into a form involving predominantly non-

negative terms in several dimensions [24]. Due to the nature of the wavefunction representation, the AFMC also deals easily with state-dependent potentials. Unfortunately, the scale of computations means that the treatment of realistic potentials will be extremely time-consuming. For certain problems, such as spin systems on a lattice, AFMC calculations appear feasible. For general multidimensional systems, however, the AFMC approach lies at the limit of presently available computer facilities. The development of more powerful stochastic techniques for many-fermion problems therefore remains a major conceptual challenge in this field.

## REFERENCES


1. M. H. KALOS, D. LEVESQUE, AND L. VERLET, *Phys. Rev. A* **9** (1974), 2178.
2. D. CEPERLEY AND M. H. KALOS, *in* "Monte-Carlo Methods in Statistical Physics" (K. Binder, Ed.), p. 149, Springer-Verlag, New York, 1979, and references cited therein.
3. D. M. CEPERLEY AND B. ALDER, *Phys. Rev. Lett.* **45** (1980), 566.
4. J. G. ZABOLITSKY AND M. H. KALOS, *Nucl. Phys. A* **356** (1981), 114.
5. D. M. ARNOW, M. H. KALOS, M. A. LEE, AND K. E. SCHMIDT, *J. Chem. Phys.* **77** (1982), 5562.
6. P. J. REYNOLDS, D. M. CEPERLEY, B. J. ALDER, AND W. A. LESTER, *J. Chem. Phys.* **77** (1982), 5593.
7. S. E. KOONIN, G. SUGIYAMA, AND H. FRIEDRICH, *in* "Time-Dependent Hartree–Fock and Beyond" (K. Goeke and P. G. Reinhard, Eds.), p. 214, Springer-Verlag, New York, 1982.
8. S. E. KOONIN, *in* "Nuclear Theory 1981" (G. Bertsch, Ed.), Proceedings, Nuclear Theory Summer Workshop, Santa Barbara, California, 1981, World Scientific, Singapore, 1982.
9. Y. AVISHAI AND J. RICHERT, *Phys. Rev. Lett.* **50** (1983), 1175.
10. J. HUBBARD, *Phys. Lett.* **3** (1959), 77; R. D. STRATONOVICH, *Dokl. Akad. Nauk. SSSR* **115** (1957), 1907 [transl.: *Soviet Phys. Dokl.* **2** (1958), 416].
11. J. E. HIRSCH, *Phys. Rev. B* **28** (1983), 4059; J. E. HIRSCH, R. L. SUGAR, D. J. SCALAPINO, AND R. BLANKENBECKLER, *Phys. Rev. B* **26** (1982), 5035.
12. S. LEVIT, *Phys. Rev. C* **21** (1980), 1594.
13. S. LEVIT, J. W. NEGELE, AND Z. PALTIEL, *Phys. Rev. C* **21** (1980), 1603.
14. J. W. NEGELE, *Rev. Modern Phys.* **54**(4) (October, 1982).
15. J. KOGUT ET AL., *Phys. Rev. Lett.* **48** (1982), 1140, and references cited therein.
16. P. BONCHE, S. E. KOONIN, AND J. W. NEGELE, *Phys. Rev. C* **13** (1976), 1226.
17. R. VARGA, "Matrix-Iterative Analysis," p. 195, Prentice–Hall, Englewood Cliffs, N.J., 1962.
18. N. METROPOLIS, A. W. ROSENBLUTH, M. N. ROSENBLUTH, A. M. TELLER, AND E. TELLER, *J. Chem. Phys.* **21** (1953), 1087.
19. R. BLANKENBECLER, R. SUGAR, AND D. SCALAPINO, *Phys. Rev. D* **24** (1981), 2278.
20. K. BINDER, *in* "Monte-Carlo Methods in Statistical Physics" (K. Binder, Ed.), p. 1, Springer-Verlag, New York, 1979.
21. B. YOON AND J. W. NEGELE, *Phys. Rev. A* **16** (1976), 1451.
22. D. BRINK, *in* "Proceedings, International School of Physics, Enrico Fermi Course XXXVI, 1966."
23. B. SEROT, S. E. KOONIN, AND J. W. NEGELE, *Phys. Rev. C* **28** (1983), 1679.
24. J. W. NEGELE, *in* "Time-Dependent Hartree–Fock and Beyond" (K. Goeke and P. G. Reinhard, Ed.), p. 198, Springer-Verlag, New York, 1982.